Journal of Mechanics, 2021, **37**, 327–332
DOI: 10.1093/jom/ufaa028
Regular Article

Stress intensity factors for cusp-type crack problem under mechanical and thermal loading

F.M. Chen[1], C.K. Chao[2,*], C.C. Chiu[2] and N.A. Noda[3]

[1]Department of Mechanical Engineering, Nan Kai University of Technology, Nantou County, Taiwan, Caotun, Republic of China
[2]Department of Mechanical Engineering, National Taiwan University of Science and Technology, Taipei, Taiwan, Republic of China
[3]Department of Mechanical Engineering, Kyushu Institute of Technology, Fukuoka, Japan

*Corresponding author: ckchao@mail.ntust.edu.tw

ABSTRACT

The general solutions of the stress intensity factors (SIFs) for a cusp-type crack problem under remote uniform mechanical and thermal loads are presented in this work. According to the complex variable theory and the method of conformal mapping, a symmetric airfoil crack is mapped onto a unit circle, and both the temperature and stress potentials are used to solve the relevant boundary-value problems. By introducing the auxiliary function and applying the analytical continuation theorem, the SIFs at the cusp-type crack tip can be analytically determined. The obtained SIF results are dependent on the geometric configurations of the cusp-type crack components and the magnitudes of the mechanical and thermal loads. For some combinations of combined loads, the SIF is maximized, and the system has a high risk of damage.

KEYWORDS: stress intensity factors, conformal mapping, analytical continuation

1. INTRODUCTION

Nearly a century ago, Inglis [1] obtained the solution of a cracked plate using elliptic coordinates. Since then, numerous related crack problems with different loading conditions and crack configurations have been investigated by many researchers. Muskhelishvili [2] obtained a general solution of the two-dimensional (2D) elasticity crack problems using the analytical continuation theorem, which is the most powerful method for solving mixed boundary-value problems. For 2D linear elasticity problems with awkwardly shaped geometries, one of the most useful techniques is to transform the region into one with a simple shape. On the basis of conformal mapping combined with the Muskhelishvili formulation for plane elasticity, many numerical solutions and techniques for the crack problem [3–10] have been developed. For example, the solution for an elliptic hole embedded in an infinite plate can be easily obtained via the mapping $z = c\cosh\ \zeta$. A simple illustration of conformal mapping combined with analytical continuation is the classical problem of an infinite plate containing an internal crack under simple tension. For this problem, the mapping function is selected as $z = m(\zeta) = (a/2)(\zeta + \zeta^{-1})$, which maps the unit circle and its exterior region in the ζ-plane onto a crack of length $2a$ and its exterior, respectively, in the z-plane. When the continuation theorem is employed, the singular points of the auxiliary function $\overline{\omega}(1/\zeta) = [m(\zeta)/\overline{m'}(1/\zeta)]\overline{\phi'}(1/\zeta) + \overline{\psi}(1/\zeta)$, which cause the continuity equation to be divergent, must be deduced such that the continuity equation can be convergent. Therefore, the structure of the proposed solution is mainly dependent on the choice of the mapping function. For example, the mapping function $m(\zeta) = (a/2)(\zeta + \zeta^{-1})$ maps a line crack of length $2a$ onto a unit circle that contains two singular points: $\zeta_1 = 1$ and $\zeta_2 = -1$. Consequently, the derivation procedure is far simpler. For the mapping function $m(\zeta) = R\zeta + (1/R\zeta)$ associated with an elliptic hole [4], there exist two singular points $\zeta_1 = (R)^{-1/2}$and$\zeta_2 = -(R)^{-1/2}$. Regarding the problem associated with a polygonal hole [5–8], the mapping function $m(\zeta) = R(\zeta + w/\zeta^n)$ with $0 \le w < 1/n$ contains $n + 1$ singular points. For example, a coated square hole problem [7] with $n = 3$ contains four singular points $\zeta_1 = (3w)^{-1/4}$, $\zeta_2 = -(3w)^{-1/4}$, $\zeta_3 = (3w)^{-1/4}i$ and $\zeta_4 = -(3w)^{-1/4}i$, which should be removed from the continuity equation. Interestingly, $w = 1/n$ in the foregoing mapping function presents a hypocycloid hole with many cusps, and a stress singularity occurs at the cusps of a hypocycloid hole. Determination of the stress intensity factors (SIFs) of a hypocycloid with many cusps in an infinite plate is important and has been carried out by many researchers [9–19]. The SIFs for both mode I and mode II at the cusp points vanish when n approaches infinity. Owing to the difference in the mapping function, the formulation of the temperature potentials and stress functions becomes even more complex, making the whole problem extremely difficult to solve.

The present study focuses on a symmetric airfoil crack in an infinite plate under combined mechanical and thermal loads. Using Muskhelishvili's complex potential method, the exact solutions of both mode-I and mode-II SIFs are presented herein. The SIF value is dependent on the magnitudes of the mechanical and thermal loads, as well as the geometric configuration of the symmetric airfoil crack. For a given geometric configuration,

Received: 27 October 2020; **Accepted:** 26 December 2020

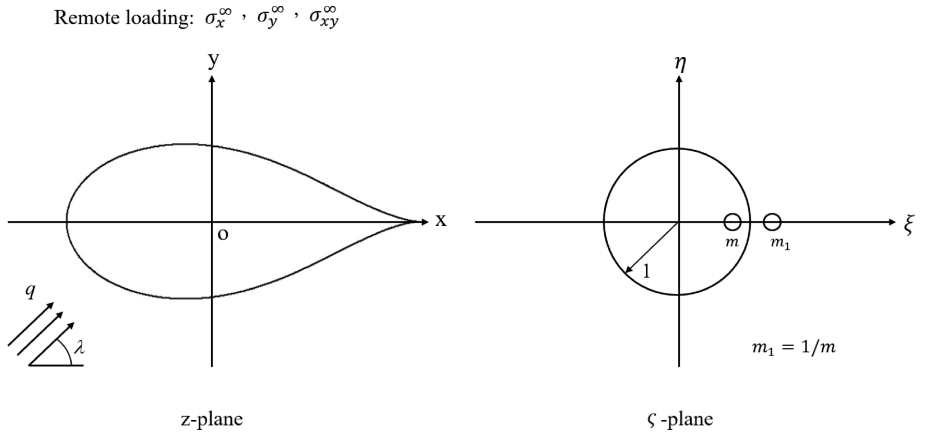

Figure 1 Mapping relation for a cusp-type crack defined by Eq. (3).

the SIF is maximized under certain combinations of combined loads, which represents the most dangerous situation. A similar problem associated with different shapes of cracks, such as a symmetric lip cusp crack, can also be treated via the proposed method.

2. PROBLEM FORMULATION

Consider a symmetric airfoil crack in an infinite plate under the remote mechanical loading denoted by σ_x^∞, σ_y^∞ and σ_{xy}^∞ and a remote uniform heat flow q forming an angle λ with the positive x-axis, as shown in Fig. 1. According to the complex variable theory for 2D plane thermoelasticity, the component of the displacement $u_x + iu_y$ and the resultant forces $-F_y + iF_x$ can be described by two complex functions $\phi(z)$ and $\psi(z)$ and a temperature potential $\theta(z) = g'(z)$, each of which is analytic in its argument $z = x + iy$, as follows:

$$2G(u_x + iu_y) = \kappa\phi(z) - z\overline{\phi'(z)} - \overline{\psi(z)} + 2G\beta \int \theta(z)\mathrm{d}z, \tag{1}$$

$$-F_y + iF_x = \phi(z) + z\overline{\phi'(z)} + \overline{\psi(z)}. \tag{2}$$

Here, G represents the shear modulus, $\kappa = 3 - 4\nu$ and $\beta = (1 + \nu)\alpha$ represent the plane strain deformation, and $\kappa = (3 - \nu)/(1 + \nu)$ and $\beta = \alpha$ represent plane stress deformation, with ν and α being the Poisson's ratio and the coefficient of thermal expansion, respectively. Here, the prime symbol represents the derivative with respect to $z = x + iy$, and the function $(\bar{\ })$ represents the complex conjugate.

To solve the relevant boundary-value problem, the conformal mapping function is introduced as follows:

$$z = w(\zeta) = \zeta + \frac{(1-m)^2}{\zeta - m}, \quad 0 \le m \le 1, \tag{3}$$

which maps the unit circle and its exterior region in the ζ-plane onto the z-plane of an airfoil crack and its exterior region. Using Eq. (3), Eqs (1) and (2) can be replaced with the following:

$$2G(u_x + iu_y) = \kappa\phi(\zeta) - \frac{w(\zeta)}{\overline{w'(\zeta)}}\overline{\phi'(\zeta)} - \overline{\psi(\zeta)} + 2G\beta \int \theta(z)\mathrm{d}z, \tag{4}$$

$$-F_y + iF_x = \phi(\zeta) + \frac{w(\zeta)}{\overline{w'(\zeta)}}\overline{\phi'(\zeta)} + \overline{\psi(\zeta)}. \tag{5}$$

To make the resulting boundary conditions as simple as possible, we introduce the following auxiliary stress function $\omega(\zeta)$:

$$\omega(\zeta) = \frac{\overline{w}(1/\zeta)}{w'(\zeta)}\phi'(\zeta) + \psi(\zeta). \tag{6}$$

3. TEMPERATURE FIELD

For a steady-state heat conduction problem, the temperature function satisfies the Laplace equation. The resultant heat flow h and temperature T are related to a complex potential $\theta(\zeta) = g'(\zeta)$, as follows:

$$T = \mathrm{Re}[\theta(\zeta)], \tag{7}$$

$$h = \int (q_x\,\mathrm{d}y - q_y\,\mathrm{d}x) = -k\,\mathrm{Im}[\theta(\zeta)], \tag{8}$$

where Re and Im represent the real and imaginary parts in Eqs (7) and (8), respectively. The quantities q_x and q_y in Eq. (8) represent the components of heat flux in the x- and y-directions, respectively, and k is the heat conductivity coefficient.

The temperature function for a symmetric airfoil crack in an infinite plate under a remote uniform heat flow can be expressed as follows:

$$\theta(\zeta) = \theta_0(\zeta) + \theta_1(\zeta), \tag{9}$$

where $\theta_0(\zeta)$ represents the unperturbed temperature field in a homogeneous plate induced by a remote uniform heat

flow and $\theta_1(\zeta)$ represents the perturbed temperature field due to the presence of a symmetric airfoil crack. To solve the relevant boundary-value problem, the unperturbed temperature field is now decomposed into two parts, as follows:

$$\theta_0(\zeta) = Qz = Q\left[\zeta + \frac{(1-m)^2}{\zeta - m}\right] = \theta_{0a}(\zeta) + \theta_{0b}(\zeta),$$
$$Q = -\frac{q}{k}e^{-i\lambda}, \tag{10}$$

where

$$\theta_{0a}(\zeta) = Q\zeta, \qquad \theta_{0b}(\zeta) = Q\frac{(1-m)^2}{\zeta - m}.$$

Note that $\theta_{0a}(\zeta)$ is holomorphic in the range of $|\zeta| < 1$, while $\theta_{0b}(\zeta)$ is holomorphic in range of $|\zeta| > 1$.

Because a symmetric airfoil crack is assumed to be insulated from the heat flow, we have

$$\mathrm{Im}[\theta(\sigma)] = 0, \quad \text{along } |\sigma| = 1. \tag{11}$$

Substituting Eqs (9) and (10) into Eq. (11) yields

$$\theta_{0a}(\sigma) + \theta_{0b}(\sigma) + \theta_1(\sigma) - \overline{\theta_{0a}(\sigma)} - \overline{\theta_{0b}(\sigma)} - \overline{\theta_1(\sigma)} = 0 \quad \text{along } |\sigma| = 1. \tag{12}$$

According to the analytical continuation theorem, Eq. (12) allows us to obtain

$$\theta_1(\zeta) = \overline{\theta_{0a}}\left(\frac{1}{\zeta}\right) - \theta_{0b}(\zeta), \quad |\zeta| \geq 1. \tag{13}$$

Substituting Eqs. (10) and (13) into Eq. (9) yields

$$\begin{aligned}\theta(\zeta) &= \theta_0(\zeta) + \theta_1(\zeta)\\ &= \theta_{0a}(\zeta) + \theta_{0b}(\zeta) + \overline{\theta_{0a}}\left(\frac{1}{\zeta}\right) - \theta_{0b}(\zeta)\\ &= \theta_{0a}(\zeta) + \overline{\theta_{0a}}\left(\frac{1}{\zeta}\right)\\ &= Q\zeta + \overline{Q}\frac{1}{\zeta}.\end{aligned} \tag{14}$$

By integrating Eq. (14) with respect to z, we can determine the temperature potential $g(\zeta)$, as follows:

$$g(\zeta) = \frac{Q\zeta^2}{2} + \overline{Q}\left(\frac{2m-1}{m^2}\right)\log\zeta - (1-m)^2\left(Q - \frac{\overline{Q}}{m^2}\right) \times \log(\zeta - m) + \left(Qm + \frac{\overline{Q}}{m}\right)\frac{(1-m)^2}{\zeta - m}. \tag{15}$$

4. STRESS FIELD

For the single-valued conditions of the traction force and the displacement, the stress functions $\phi(\zeta)$ and $\omega(\zeta)$ must take the following form:

$$\phi(\zeta) = A\log\zeta + \phi_1(\zeta) + \phi_0(\zeta), \tag{16}$$

$$\omega(\zeta) = B\log\zeta + \omega_1(\zeta) + \omega_0(\zeta), \tag{17}$$

where $\phi_0(\zeta) = \Gamma\zeta = [(\sigma_x^\infty + \sigma_y^\infty)/4]\zeta$ and $\omega_0(\zeta)$ are defined as the singular parts of $\phi(\zeta)$ and $\omega(\zeta)$, respectively, while $\phi_1(\zeta)$ and $\omega_1(\zeta)$ are the complementary parts of the complex potentials $\phi(\zeta)$ and $\omega(\zeta)$, respectively.

The constants A and B in Eqs (16) and (17), respectively, can be determined from the single-value condition of displacement and traction force, as follows:

$$2G[u_x + iu_y]_c = \kappa[\phi(\zeta)]_c - [\overline{\omega(\zeta)}]_c + 2G\beta[g(\zeta)]_c = 0, \tag{18}$$

$$[-F_y + iF_x]_c = [\phi(\zeta)]_c + [\overline{\omega(\zeta)}]_c = 0. \tag{19}$$

Here, $[f(\zeta)]_c = f(r, 2\pi) - f(r, 0)$ represents a jump when enclosing a contour. Substituting Eqs (16) and (17) into Eqs (18) and (19) and knowing that

$$[g(\zeta)]_c = 2\pi i[\overline{Q} - (1-m)^2Q], \quad [\log\zeta]_c = 2\pi i \quad \text{and} \quad [\log\overline{\zeta}]_c = -2\pi i, \tag{20}$$

we have

$$\kappa A + \overline{B} + 2G\beta[\overline{Q} - (1-m)^2Q] = 0 \tag{21}$$

and

$$A - \overline{B} = 0. \tag{22}$$

Solving for Eqs (21) and (22), we have

$$A = \frac{-2G\beta}{(1+\kappa)}[\overline{Q} - (1-m)^2Q],$$
$$B = \frac{-2G\beta}{(1+\kappa)}[Q - (1-m)^2\overline{Q}].$$

Hence, the stress functions become

$$\phi(\zeta) = \frac{-2G\beta}{(1+\kappa)}\left[-(1-m)^2Q + \overline{Q}\right]\log\zeta + \phi_0(\zeta) + \phi_1(\zeta), \tag{23}$$

$$\omega(\zeta) = \frac{-2G\beta}{(1+\kappa)}[-(1-m)^2\overline{Q} + Q]\log\zeta + \omega_0(\zeta) + \omega_1(\zeta). \tag{24}$$

From the definition of the mapping function, we have

$$\begin{aligned}\bar{w}\left(\frac{1}{\zeta}\right) &= \frac{1}{\zeta} + \frac{(1-m)^2}{\zeta^{-1} - m}\\ &= \frac{1}{\zeta} - \frac{(1-m)^2m_1^2}{\zeta - m_1} - (1-m)^2m_1\end{aligned} \quad (m_1 = 1/m > 1). \tag{25}$$

Note that the second term on the right-hand side of Eq. (25) is the singular part for $\overline{w}(1/\zeta)$ defined in the region $|\zeta| > 1$.

Therefore, $\omega_0(\zeta)$ defined as the singular part of $\omega(\zeta)$ in Eq. (6) can be expressed as

$$\omega_0(\zeta) = -\frac{(1-m)^2}{m^2}\frac{\phi'(m_1)}{w'(m_1)}\frac{1}{\zeta - m_1} + \psi_0(\zeta)$$
$$= -\frac{(1-m^2)^2(\Gamma + S)}{m^2(2m+1)}\frac{1}{\zeta - m_1} + \psi_0(\zeta), \quad (26)$$

where $\psi_0(\zeta) = \Gamma_1\zeta = [(\sigma_y^\infty - \sigma_x^\infty)/2 + i\sigma_{xy}^\infty]\zeta$ and $\phi'(m_1) = \phi'_0(m_1) + \phi'_1(m_1) = \Gamma + S$.

From Eqs (5), (6), (16) and (17), the traction-free condition along the unit circle in the ζ-plane can be expressed as follows:

$$\phi_0(\sigma) + \phi_1(\sigma) + \overline{\omega_0(\sigma)} + \overline{\omega_1(\sigma)} = 0, \quad \sigma \in L. \quad (27)$$

Note that the logarithmic term in Eq. (23) or (24) is canceled out when the traction-free condition is applied along the unit circle ($\sigma\overline{\sigma} = 1$). According to the continuation theorem, Eq. (27) allows us to obtain

$$\phi_1(\zeta) = -\overline{\omega_0}(1/\zeta) = -\frac{(1-m^2)^2(\Gamma + S)}{1+2m}\frac{1}{\zeta - m} - \overline{\Gamma_1}\frac{1}{\zeta} \quad (28)$$

and

$$\omega_1(\zeta) = -\overline{\phi_0}(1/\zeta) = -\Gamma/\zeta, \quad (29)$$

where $S = \phi_1'(m_1) = [m^2(\Gamma + S)/(1+2m)] + m^2\overline{\Gamma_1}$ and $\Gamma + S = [(1+2m)/(1+2m-m^2)](\Gamma + m^2\overline{\Gamma_1})$.

Therefore, we have

$$\phi_1(\zeta) = -\frac{(1-m^2)^2(\Gamma + m^2\overline{\Gamma_1})}{1+2m-m^2}\frac{1}{\zeta - m} - \overline{\Gamma_1}\frac{1}{\zeta}. \quad (30)$$

Hence, Eqs (23) and (24) become

$$\phi(\zeta) = \frac{-2G\beta}{(1+\kappa)}[-(1-m)^2Q + \overline{Q}]\log\zeta + \Gamma\zeta$$
$$- \frac{(1-m^2)^2(\Gamma + m^2\overline{\Gamma_1})}{1+2m-m^2}\frac{1}{\zeta - m} - \overline{\Gamma_1}\frac{1}{\zeta}, \quad (31)$$

$$\omega(\zeta) = \frac{-2G\beta}{(1+\kappa)}[-(1-m)^2\overline{Q} + Q]\log\zeta$$
$$- \frac{(1-m^2)^2(\Gamma + m^2\overline{\Gamma_1})}{m^2(1+2m-m^2)}\frac{1}{\zeta - m_1} + \Gamma_1\zeta - \Gamma\frac{1}{\zeta}. \quad (32)$$

For the special case of a circular hole ($m = 1$), the foregoing stress functions are reduced to the following:

$$\phi(\zeta) = \frac{-2G\beta\overline{Q}}{(1+\kappa)}\log\zeta + \Gamma\zeta - \overline{\Gamma_1}\frac{1}{\zeta}, \quad (33)$$

$$\omega(\zeta) = \frac{-2G\beta Q}{(1+\kappa)}\log\zeta + \Gamma_1\zeta - \Gamma\frac{1}{\zeta}, \quad (34)$$

which are in agreement with the results of Chao and Shen [20].

To determine the SIF at tip A, the following definition is used:

$$K_1 - iK_2 = \lim_{z\to a} 2\sqrt{2\pi\{w(\zeta) - w(1)\}}\frac{\phi'(1)}{w'(\zeta)}. \quad (35)$$

In view of the mapping function, the crack length is determined as $a = 2$ by setting $m = 0$, and the SIFs at tip A defined in Eq. (35) can be replaced with the following:

$$K_1 - iK_2 = \sqrt{1-m}\sqrt{\pi a}\phi'(1), \quad (36)$$

where

$$\phi'(1) = \frac{-2G\beta}{(1+\kappa)}[-(1-m)^2Q + \overline{Q}] + \Gamma$$
$$+ \frac{(1+m)^2(\Gamma + m^2\overline{\Gamma_1})}{1+2m-m^2} + \overline{\Gamma_1}. \quad (37)$$

For a line crack with length $2a$ embedded in an infinite plate subjected to a remote uniform heat flow, the SIFs at tip A are given as follows:

$$K_1 = 0, \quad K_2 = \frac{-2G\beta qa\sqrt{\pi a}}{(1+\kappa)k}\sin\lambda, \quad (38)$$

which are in agreement with the results of Sih [21].

For an isothermal case, the expression for the SIFs at tip A is reduced to

$$K_1 - iK_2 = \sqrt{1-m}\sqrt{\pi a}\left[\frac{(4m+2)}{1+2m-m^2}\Gamma\right.$$
$$\left. + \frac{m^4 + 2m^3 + 2m + 1}{1+2m-m^2}\overline{\Gamma_1}\right], \quad (39)$$

which is identical to the result of Chen [16].

5. NUMERICAL EXAMPLES

The SIFs for a symmetric airfoil crack are dependent on the loading conditions and geometric configurations through the function $\varphi'(1)$ defined by Eq. (37). The SIFs at tip A for a simple example of a line crack were obtained from our results by setting $m = 0$ in Eq. (39). In the following examples, we aim to determine the SIFs for several loading conditions and different geometric configurations. The plots of different geometric configurations for a symmetric airfoil crack with different values of m are shown in Fig. 2.

5.1 Combined mechanical loading ($\sigma_x^\infty = \sigma_0, \sigma_y^\infty = \sigma_{xy}^\infty = 0$) and thermal loading ($\lambda = 0^0$)

Considering $\sigma_x^\infty = \sigma_0$, $\sigma_y^\infty = \sigma_{xy}^\infty = 0$ and $\lambda = 0^0$, we have $\Gamma = \sigma_0/4$, $\Gamma_1 = -\sigma_0/2$ and $Q = -q/k$, and from Eqs (36) and (37), we obtain

$$K_1 = \sqrt{1-m}\sqrt{\pi a}\left[(2m - m^2)\frac{G\beta qa}{(1+\kappa)k}\right.$$
$$\left. - \frac{m^2(m^2+2m)}{2(1+2m-m^2)}\sigma_0\right], \quad K_2 = 0. \quad (40)$$

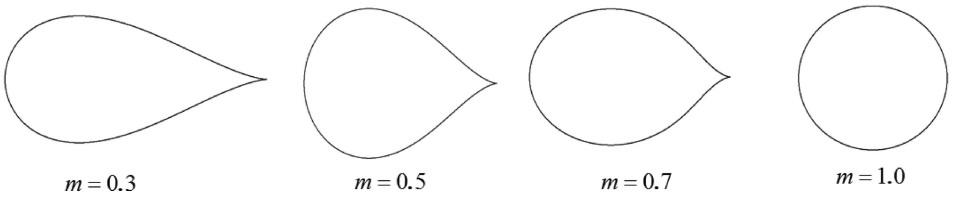

Figure 2 Geometric configurations of a symmetric airfoil crack for different values of m.

5.2 Combined mechanical loading ($\sigma_y^\infty = \sigma_0, \sigma_x^\infty = \sigma_{xy}^\infty = 0$) and thermal loading ($\lambda = 0^0$)

Considering $\sigma_y^\infty = \sigma_0, \sigma_x^\infty = \sigma_{xy}^\infty = 0$ and$\lambda = 0^0$, we have $\Gamma = \sigma_0/4$, $\Gamma_1 = \sigma_0/2$ and $Q = -q/k$, and from Eqs (36) and (37), we obtain

$$K_1 = \sqrt{1-m}\sqrt{\pi a}\left[(2m-m^2)\frac{G\beta qa}{(1+\kappa)k} + \frac{m^4+2m^3+4m+2}{2(1+2m-m^2)}\sigma_0\right], \quad K_2 = 0. \tag{41}$$

5.3 Combined mechanical loading ($\sigma_y^\infty = \sigma_0, \sigma_x^\infty = \sigma_{xy}^\infty = 0$) and thermal loading ($\lambda = 180^0$)

Considering $\sigma_y^\infty = \sigma_0, \sigma_x^\infty = \sigma_{xy}^\infty = 0$ and $\lambda = 180^0$, we have $\Gamma = \sigma_0/4$, $\Gamma_1 = \sigma_0/2$ and $Q = q/k$, and from Eqs (36) and (37), we obtain

$$K_1 = \sqrt{1-m}\sqrt{\pi a}\left[-(2m-m^2)\frac{G\beta qa}{(1+\kappa)k} + \frac{m^4+2m^3+4m+2}{2(1+2m-m^2)}\sigma_0\right], \quad K_2 = 0. \tag{42}$$

5.4 Combined mechanical loading ($\sigma_{xy}^\infty = \sigma_0, \sigma_x^\infty = \sigma_y^\infty = 0$) and thermal loading ($\lambda = 90^0$)

Considering $\sigma_{xy}^\infty = \sigma_0, \sigma_x^\infty = \sigma_y^\infty = 0$ and $\lambda = 90^0$, we have $\Gamma = 0$, $\Gamma_1 = i\sigma_0$ and $Q = iq/k$, and from Eqs (36) and (37), we obtain

$$K_1 = 0,$$

$$K_2 = \sqrt{1-m}\sqrt{\pi a}\left[-(m^2-2m+2)\frac{G\beta qa}{(1+\kappa)k} + \frac{m^4+2m^3+2m+1}{1+2m-m^2}\sigma_0\right]. \tag{43}$$

According to the foregoing numerical results, the following important conclusions can be drawn:

(1) When the cusp-type crack components are subjected to tension loading σ_0 along the x-axis and a remote heat flow q approaches from the negative x-axis ($\lambda = 0^0$), the K_1 value at tip A will become negative if the magnitude of the tension loading σ_0 is sufficiently large that $[(1+\kappa)k\sigma_0]/G\beta qa > [2(1+2m-m^2)(2m-m^2)]/[m^2(m^2+2m)]$, as shown in Fig. 3.

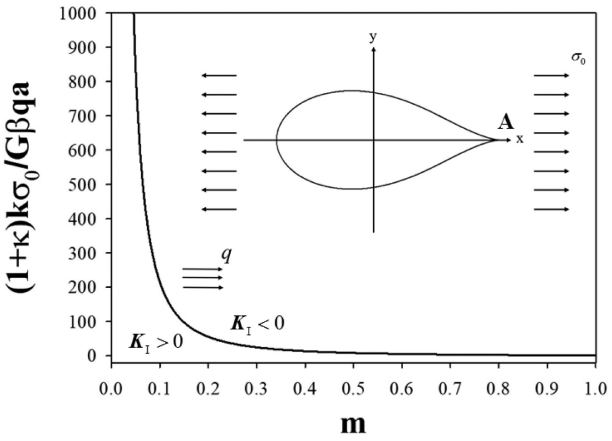

Figure 3 Crack propagation criterion for the cusp-type crack components subjected to tension loading σ_0 along the x-axis and a remote heat flow q approaching from the negative x-axis.

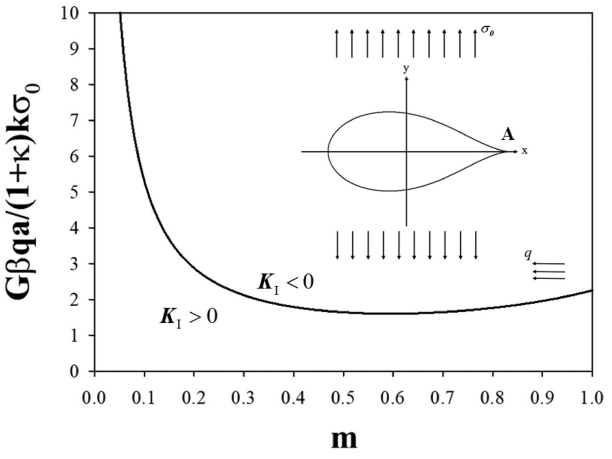

Figure 4 Crack propagation criterion for the cusp-type crack components subjected to tension loading σ_0 along the y-axis and a remote heat flow q approaching from the positive x-axis.

(2) When the cusp-type crack components are subjected to tension loading σ_0 along the y-axis and a remote heat flow q approaches from the negative x-axis ($\lambda = 0^0$), the K_1 value at tip A is always positive, regardless of the magnitude of the tension loading σ_0 and the strength of heat flow q, which places the components in a dangerous situation.

(3) When the cusp-type crack components are subjected to tension loading σ_0 along the y-axis and a remote heat

flow q approaches from the positive x-axis ($\lambda = 180^0$), crack propagation of the components will be suppressed if the strength of the heat flux is sufficiently large that $G\beta qa/[(1+\kappa)k\sigma_0] > (m^4+2m^3+4m+2)/[2(1+2m-m^2)(2m-m^2)]$, as shown in Fig. 4.

(4) When the cusp-type crack components are subjected to a shear load σ_0 and a remote heat flow q approaches from the negative y-axis ($\lambda = 90^0$), the K_1 value at tip A always vanishes, and the K_2 value at tip A becomes

$$K_2 = \sqrt{1-m}\sqrt{\pi a}\left[-(m^2-2m+2)\frac{G\beta qa}{(1+\kappa)k} + \frac{m^4+2m^3+2m+1}{1+2m-m^2}\sigma_0\right].$$

6. CONCLUDING REMARKS

An exact solution of the SIFs for a symmetric airfoil crack under combined mechanical and thermal loads is presented. The solution is based on the method of analytical continuation in conjunction with conformal mapping. The obtained results indicate that when the cusp-type crack components are subjected to a tension load σ_0 along the y-axis and a remote heat flow q approaches from the negative x-axis ($\lambda = 0^0$), the K_1 value at tip A always becomes positive regardless of the magnitude of the tension loading σ_0 and the strength of the heat flow q, which places the components in a dangerous situation. However, when the cusp-type crack components are subjected to a tension loading σ_0 along the y-axis and a remote heat flow q approaches from the positive x-axis ($\lambda = 180^0$), crack propagation of the components is suppressed if the strength of the heat flux is sufficient that $G\beta qa/[(1+\kappa)k\sigma_0] > (m^4+2m^3+4m+2)/[2(1+2m-m^2)(2m-m^2)]$.

ACKNOWLEDGEMENT

The research was supported by the Ministry of Science and Technology of Taiwan under grant MOST 109-2221-E-011-009-MY3.

REFERENCES

1. Inglis CE. Stresses in a plate due to the presence of cracks and sharp corners. *Transactions of the Royal Institute of Naval Architects* 1913;**60**:219–241.
2. Muskhelishvili NI. *Some Basic Problems of the Mathematical Theory of Elasticity*. Groningen, The Netherlands: P. Noordhoff Ltd, 1953.
3. Chen YZ. Elastic analysis of an infinite plate containing hole with cusps and applied by concentrated forces. *Engineering Fracture Mechanics* 1964;**20**:573–582.
4. Chao CK, Lu LM, Chen CK, Chen FM. Analytical solution for a reinforcement layer in a coated elliptic hole under a remote uniform load. *International Journal of Solids and Structures* 2009;**46**: 2959–2965.
5. Chao CK, Tseng SC, Chen FM. An analytical solution to a coated triangular hole embedded in an infinite plate under a remote uniform heat flow. *Journal of Thermal Stresses* 2018;**41**:1259–1275.
6. Tseng SC, Chao CK, Chen FM. Stress field for a coated triangle-like hole problem in plane elasticity. *Journal of Mechanics* 2020;**36**: 55–72.
7. Tseng SC, Chao CK, Chen FM. Interfacial stresses of a coated square hole induced by a remote uniform heat flow. *International Journal of Applied Mechanics* 2020;**12**:2050063.
8. Tseng SC, Chao CK, Chen FM, Chiu WC. Interfacial stresses of a coated polygonal hole under a point heat source. *Journal of Thermal Stresses* 2020;**43**:1259–1275.
9. Wu CH. Unconventional internal cracks, part I: symmetric variations of a straight crack. *ASME Journal of Applied Mechanics* 1982;**49**:62–68.
10. Chen YZ. Closed form solutions of T-stress in plane elasticity crack problems. *International Journal of Solids and Structures* 2000;**37**:1629–1637.
11. Nik Long NMA, Yaghobifar M. General analytical solution for stress intensity factor of hypocycloid hole with many cusps in an infinite plate. *Philosophical Magazine Letters* 2011;**91**:256–263.
12. Wu X, Schiavone P. Finite deformation of harmonic solids with cusp cracks. *IMA Journal of Applied Mathematics* 2014;**79**:790–803.
13. Sharma DS, Dave JM. Stress intensity factors for hypocycloidal hole with cusps in infinite anisotropic plate. *Theoretical and Applied Fracture Mechanics* 2015;**75**:44–52.
14. Chauhan MM, Sharma DS, Dave JM. Stress intensity factor for hypocycloidal hole with cusps in finite plate. *Theoretical and Applied Fracture Mechanics* 2016;**82**:59–68.
15. Shahzad S, Corso FD, Bigoni D. Hypocycloidal inclusions in nonuniform out-of-plane elasticity: stress singularity vs stress reduction. *Journal of Elasticity* 2017;**126**:215–229.
16. Chen YZ. Fracture analysis for a cusp-type crack problem. *Acta Mechanica* 2020;**231**:3123–3128.
17. Noda NA, Li R, Miyazaki R, Takaki R, Sano Y. Convenient adhesive strength evaluation method in terms of the intensity of singular stress field. *International Journal of Computational Methods* 2019;**16**:1–28.
18. Zhu N, Oterkus E. Calculation of stress intensity factor using displacement extrapolation method in peridynamic framework. *Journal of Mechanics* 2020;**36**:235–243.
19. Ramalho L, Belinha J, Campilho RDSG. A new crack propagation algorithm combined with the finite element method. *Journal of Mechanics* 2020;**36:**405–422.
20. Chao CK, Shen MH. On bonded circular inclusions in plane thermoelasticity. *ASME Journal of Applied Mechanics* 1997;**64**:1000–1004.
21. Sih GC. On the singular character of thermal stresses near a crack tip. *ASME Journal of Applied Mechanics* 1962;**29**:587–589.